

Article

Identification and Expression Pattern of the Carotenoid Cleavage Oxygenase Gene Family in *Lycium* Suggest CCOs Respond to Abiotic Stress and Promote Carotenoids Degradation

Weinan Li ^{1,2}, Jiahang Che ^{1,2}, Qile Lian ^{1,2}, Cuiping Wang ³, Guoli Dai ⁴ and Jinhuan Chen ^{1,2,*} ¹ College of Biological Sciences and Technology, Beijing Forestry University, Beijing 100083, China² Key Laboratory of Genetics and Breeding in Forest Trees and Ornamental Plants, Ministry of Education, Beijing Forestry University, Beijing 100083, China³ School of Biological Science and Engineering, North Minzu University, Yinchuan 750021, China⁴ National Wolfberry Engineering Research Center, Ningxia Academy of Agriculture and Forestry Sciences, Yinchuan 750002, China

* Correspondence: chenjh@bjfu.edu.cn

Abstract: Carotenoids are key metabolites in goji (*Lycium*), a traditional Chinese medicine plant; however, the carotenoid content varies in fruits of different goji species, and the mechanism of this variation is not clear. Carotenoids participate in signal transduction and photosynthesis, and function as colorants and photoprotectors. Members of the carotenoid cleavage oxygenase (CCO) gene family are involved in the regulation of phytohormones, pigments, and aromatic substances, such as abscisic acid (ABA), β -carotenoid, and α -ionone, by degrading carotenoids. Some CCO genes are also related to an abiotic stress response. Here, a total of 12 *LbCCO* genes were identified and analyzed from the *L. barbarum* genome. CCO genes were divided into six subfamilies based on the constructed phylogenetic tree, including *LbNCEDs*, *LbCCD1*, *LbCCD3*, *LbCCD4*, *LbCCD7*, and *LbCCD8*. Among them, *CCD3* was reported for the first time. The gene structure and motif analysis revealed the conservation of CCO subfamilies. Pseudogene generation and the importance of each subfamily in CCOs were revealed by collinearity analysis. The spatiotemporal transcriptomes of *L. barbarum* and *L. ruthenicum* were compared, suggesting that *CCD4-1* may dominate carotenoid degradation in goji fruits. *Cis*-acting elements prediction and environment responsive gene expression analyses indicated that salt-alkali stress and photothermal conditions might influence the expression of CCOs in goji. The results of this study enhance our understanding of the carotenoid degradation pathway, and the functions and responses of CCOs in goji species.

Keywords: carotenoid cleavage oxygenase; gene family; stress; goji; express pattern

Citation: Li, W.; Che, J.; Lian, Q.; Wang, C.; Dai, G.; Chen, J. Identification and Expression Pattern of the Carotenoid Cleavage Oxygenase Gene Family in *Lycium* Suggest CCOs Respond to Abiotic Stress and Promote Carotenoids Degradation. *Forests* **2023**, *14*, 983. <https://doi.org/10.3390/f14050983>

Academic Editor: John E. Carlson

Received: 28 March 2023

Revised: 5 May 2023

Accepted: 6 May 2023

Published: 10 May 2023



Copyright: © 2023 by the authors. Licensee MDPI, Basel, Switzerland. This article is an open access article distributed under the terms and conditions of the Creative Commons Attribution (CC BY) license (<https://creativecommons.org/licenses/by/4.0/>).

1. Introduction

There are more than 80 species of *Lycium* in the world [1], with seven species found in China [2]. Of these species, *L. barbarum* and *L. ruthenicum* contain numerous phytochemicals including polysaccharides, betaine, phenolics, carotenoids, cerebroside, ascorbic acid, beta-sitosterol, flavonoids, anthocyanins, and vitamins, and have been used for medicinal purposes for thousands of years [3]. The fruits of these two goji species contain dramatically varied amounts of carotenoids [4], indicating potential differences in their carotenoid metabolism processes.

Carotenoids are isoprenoid-based pigments with various functions among bacteria, fungi, plants, and animals [5,6], and are considered as important sources of nutrition for humans and other animals. Carotenoids are precursors of vitamin A, photo-protectors, and antioxidants, enhancers of immunity, and contributors to reproduction [7]. In plants, carotenoids participate in signal transduction and photosynthesis and function as colorants

and photoprotectors. Carotenoids can be oxidized by carotenoid cleavage oxygenases (CCOs) into bioactive substances with specific functions, such as volatile flavor compounds and hormones including abscisic acid (ABA) and strigolactone (SL) [8–10]. ABA is a major phytohormone that regulates plant growth, development, responses to different kinds of stresses, and a variety of adaptation processes, such as seed dormancy, growth restriction, and leaf senescence [6,11,12]. Strigolactone helps plants sense nutrient availability, especially phosphate and minimize shoot growth and increase the root area to accumulate nutrition, and promotes arbuscular mycorrhizal fungi symbiosis to acquire inorganic nutrients [6,13,14].

In previous studies, CCOs were grouped into six subfamilies, including five types of carotenoid cleavage dioxygenases (CCDs, *CCD1*, 2, 4, 7, 8) and 9-*cis*-epoxycarotenoid dioxygenases (NCEDs) with various functions [8,15]. CCDs generate apocarotenoids through a carotenoid oxidative cleavage process [9]. *CCD1* functions in the cleavage of carotene, zeaxanthin, and apocarotenoids for the synthesis of apocarotenoid flavor and aroma volatiles, such as α -ionone [16–19]. *CCD4* acts to produce β -cyclocitral or β -ionone through the cleavage of β -carotene in different ways, making *CCD4* a potential determinant of fruit or flower color [20–23]. Lycopene and β -xanthophylls (β -cryptoxanthin, zeaxanthin) were identified as substrates of *CCD4* [20,21]. *CCD7* and *CCD8* are involved in the synthesis of strigolactone and then regulate shoot and root branching or interact with soil microbes [22]. NCEDs encode rate-limiting enzymes in the biosynthesis of ABA and cleaved 9-*cis*-epoxycarotenoids produce direct precursors of ABA in higher plants [23]. NCEDs regulate plant development, senescence, and response to abiotic stress by regulating ABA accumulation. The overexpression of *LeNCED1* can promote salt accumulation in leaves and xylem sap to help minimize plant growth loss under salt stress [24]. Increasing the ABA level was found to be related to the expression of *NCED1* under drought stress in plants such as *Aristotelia chilensis* [25]. The expression of *NCED1* was related to carotenoid degradation in kiwifruit [26]. *VviNCED2* and *VviNCED3* increased the ABA level in response to cold stress [27]. *GaNCED3a* can enhance the drought resistance of cotton [28]. Through being constitutively expressed in various tissues in *Oryza sativa*, *OsNCED3* can regulate seed germination and seedling growth by controlling ABA content [29].

Although abiotic stress, including salt-alkali and high temperature, can adversely affect plant growth and development, it also promotes the accumulation of functional phytochemicals in plants [30]. Under salt stress, tomato plants can uptake and transport significant amounts of Na^+ to the shoot, resulting in enhanced organoleptic properties of the tomato fruits, as evidenced by increases in carotenoids, flavonoids, vitamin C, total phenolic compounds, total soluble solids, and total titratable acids [31]. High light intensity and high temperature stress induced chlorophyll loss and the synthesis of carotenoids in tomato plants [32]. Carrots under salt and simulated drought conditions exhibit an overall or partial increase in carotenoid content [33,34].

L. barbarum is rich in carotenoids, with amounts reported to be as high as 233 $\mu\text{g/g}$ DW in fruit [35]. However, little is known about carotenoid synthesis and the related metabolic pathways in this species. *L. barbarum* and *L. ruthenicum* fruits differ significantly in carotenoid content, with *L. barbarum* being rich in carotenoids in mature fruits and *L. ruthenicum* fruits containing almost no carotenoids [35]. To date, the genes responsible for this variation in carotenoid synthesis or degradation between *L. barbarum* and *L. ruthenicum* have not been determined. A previous study suggested the influences of both carotenoid synthesis and carotenoid degradation processes on the carotenoid content [36]. In this study, we investigated the CCO gene family of *L. barbarum* and performed the evolutionary analysis to predict the classification of LbCCOs. We then performed a bioinformatics analysis of the structure, conserved domains, motifs, and promoters of the identified genes. Finally, we analyzed and compared the expression patterns of the CCOs in *L. barbarum* and *L. ruthenicum* in different spaces and times and analyzed the expression patterns under different environment conditions.

2. Materials and Methods

2.1. Plant Materials

Three-year-old *L. barbarum* and *L. ruthenicum* seedling clones were cultivated in 38°38'51" N, 106°9'29" E. Stamens, pistils, green fruits, mature fruits, leaves on current year branches, leaves on last year branches, and stem tips were collected. Each kind of material was collected in June 2021 with three biological replicates from three different trees under normal cultivation and management conditions of goji. Three-year-old *L. barbarum* clones were cultivated in 38°38'51" N, 106°9'29" E (Yinchuan, Ningxia) at 1070 m above sea level and 36°26'3" N, 96°25'35" E (Nomhon, Qinghai) at 2750 m above sea level. Weather data were recorded in Nomhon and Yinchuan by a weather station with multiple sensors, and included average high and low temperature, hours of daylight and twilight, and average daily incident shortwave solar energy. Green and red (mature) fruits were collected in July 2022 with three biological replicates from three different trees under normal cultivation and management conditions of goji. All samples were immediately frozen in liquid nitrogen after collection and all samples were stored at −80 °C before testing.

2.2. Identification of LbCCO Family Genes

The whole genome sequence of *L. barbarum* (GenBank assembly accession: GCA_019175385.1) was downloaded from the NCBI database. RPE65 (retinal pigment epithelial membrane protein) is a conserved structural domain of the CCO gene family [37]. To identify all the CCOs, the HMM (hidden Markov model) profile of the RPE65 domain (PF03055 in Pfam protein database), a statistical model of the primary structure consensus of a sequence family, was used to search against the *L. barbarum* genome in TBtools [38]. RPE65 domain verification for the protein sequences was performed using SMART [39,40] and NCBI-CCD [41] databases, and genes that encoded proteins with less than 150 amino acids in the RPE65 domain were identified as genes with an incomplete conservative domain and then were filtered out.

2.3. Classification and Protein Characterization of LbCCOs

CCO family genes from *Arabidopsis thaliana*, *Nicotiana tabacum*, *Solanum lycopersicum*, *L. ruthenicum*, and *Crocus sativus* were collected as reference genes, and their amino acid sequences were downloaded from the NCBI protein (<https://www.ncbi.nlm.nih.gov/protein>, accessed on 20 April 2022), Swiss-Prot [42], or TAIR [43] databases. A maximum likelihood phylogeny tree (ML tree) was constructed by Tbttools-One Step Build a ML tree with the CCO protein sequences from the identified genes and reference genes using default parameters [38]. The interactive tree of life (iTOL, <https://itol.embl.de/>, accessed on 20 April 2022) was used to visualize the ML tree. Gene symbols of *L. barbarum* CCOs were named, referring to the symbols of genes that clustered into the same class in the ML tree.

Physicochemical properties, including the MW (molecular weight), pI (isoelectric point), instability index, aliphatic index, and GRAVY (grand average of hydropathicity) of LbCCOs were calculated and predicted by ExPASy-ProtParam (<https://web.expasy.org/protparam/>, accessed on 20 April 2022) [44]. Subcellular localizations of CCO proteins were predicted by TargetP-2.0 (<https://github.com/JJAlmagro/TargetP-2.0/>, accessed on 20 April 2022).

2.4. Analysis of Gene Structure and Cis-Acting Elements of Identified LbCCOs

Conserved motifs and RPE65 domains were analyzed with default parameters in Tbttools-Simple MEME Wrapper and the NCBI-CCD database [38], respectively. Cis-acting elements in the promoter prediction was performed in PlantCARE (<https://bioinformatics.psb.ugent.be/webtools/plantcare/html/>, accessed on 20 April 2022) and then visualized by Tbttools software [38].

2.5. Chromosome Localization, Gene Density, and Collinearity Analysis of *LbCCOs*

Chromosome localization, gene density, and collinearity analysis were constructed and visualized using Tbtools with default parameters [38]. Collinearity analysis of *LbCCOs* was calculated by One Step MCScanX of Tbtools [38], retaining results with e-values less than 1×10^{-10} and keeping five blast hits.

2.6. Expression Patterns of *LbCCOs*

L. barbarum and *L. ruthenicum* fruit developmental RNA-Seq data (green fruit, color changing, and ripening stages) were filtered from raw data obtained from NCBI-SRA (accession number: PRJNA483521) [45]. High-quality reads (clean reads) were obtained by removing adapter sequences and eliminating reads containing more than 10% unknown nucleotides and low-quality reads (reads containing more than 50% bases with a Q-value ≤ 20). *L. ruthenicum* stress transcriptome RNA-Seq data (raw data) were obtained from NCBI-SRA (accession number: PRJNA285517). Gene expression levels of fruits in Ningxia and Qinghai were determined from transcriptome data.

Gene expression levels of stamens, pistil, green fruit, mature fruit, leaves on current year branches, leaves on last year branches, and stem tips of the two goji species were determined from transcriptome data. Transcriptome analysis was performed as follows: total RNA was extracted from plant samples using the RNAPrep Pure Plant Kit (Tiangen, Beijing, China) according to the instructions. The RNA concentration and purity were measured using NanoDrop 2000 (Thermo Fisher Scientific, Wilmington, DE, USA). The RNA integrity was assessed using the RNA Nano 6000 Assay Kit of the Agilent Bioanalyzer 2100 system (Agilent Technologies, Santa Clara, CA, USA). A total amount of 1 μ g RNA per sample was used as input material. Sequencing libraries were generated using NEBNext Ultra™ RNA Library Prep Kit for Illumina (NEB, Ipswich, MA, USA). For this, mRNA was purified from total RNA using poly-T oligo-attached magnetic beads. Following purification, the mRNA was fragmented into small pieces using divalent cations at an elevated temperature. Cleaved RNA fragments were reverse-transcribed to create the final cDNA library in accordance with the protocol for the mRNA-Seq sample preparation kit. To select cDNA fragments that were 240 bp in length, the library fragments were purified with AMPure XP system (Beckman Coulter, Brea, CA, USA). Library quality was assessed on the Agilent Bioanalyzer 2100 system and sequenced on an Illumina platform, and paired-end reads were generated.

Fastp (<https://github.com/OpenGene/fastp>, accessed on 15 March 2023) was used to obtain clean reads from raw data with default parameters. Kallisto (<https://github.com/pachterlab/kallisto>, accessed on 15 March 2023) was used to determine the gene expression level with parameters.

2.7. Gene and Promoter Isolation

Plant tissues from *L. barbarum* and *L. ruthenicum* seedlings were transferred to mortar, milled to a powder, and mixed with liquid nitrogen immediately. The Plant Genomic DNA Kit (Tiangen, China) and RNAPrep Pure Plant Kit (Tiangen, China) were used to extract DNA and RNA, respectively. After checking the RNA quality, the FastKing RT Kit (Tiangen, China) was used to reversely transcribe RNA to cDNA.

The sequences of *CCD4-1s* and their promoters were obtained from the goji genome or public database and primers (Supplemental Table S1) were designed by Primer3Plus (<https://www.primer3plus.com/>, accessed on 19 November 2021) to use PCR to amplify the *CCD4-1s* coding region and *CCD4-1* promoters. After purification by TIANgel Purification Kit (Tiangen, China), the PCR products were cloned into the pMD18-T vector and sequenced. The gene and promoter sequences of *L. barbarum* and *L. ruthenicum* were compared. Binding site prediction was performed on the Plant Transcriptional Regulatory Map (http://plantregmap.gao-lab.org/binding_site_prediction.php, accessed on 19 August 2022) website using *A. thaliana* transcription factors as the model.

2.8. Subcellular Localization

LbCCD4-1 and *LrCCD4-1* coding regions without stop codons were inserted into the pBI121 vector and then fused with the *EGFP* gene to construct plasmids encoding CCD4-1-EGFPs. The plasmids were separately introduced into *Agrobacterium tumefaciens* strain GV3101 by the freeze-thaw method and then transformed into *Nicotiana benthamiana* leaf cells using the agrobacterium infection method. The tobacco plants were grown in the dark for 1 day, with normal light cultivation for 2 day, and then imaged by TCS SP8 X confocal microscopy (Leica, Germany) using a 488-nm laser line to image EGFP and chloroplast signal.

3. Results

3.1. Identification and Classification of LbCCOs

The *L. barbarum* genome sequence was obtained from the NCBI database (GenBank assembly accession: GCA_019175385.1). The retinal pigment epithelial membrane protein domain (RPE65 domain) is a conserved structure of carotenoid cleavage oxygenase [37]. To identify *LbCCO* members, an HMM search was conducted with the RPE65 HMM profile downloaded from the Pfam protein database. A total of 19 putative *LbCCOs* were detected. NCBI-CCD and SMART were then used to filter genes lacking RPE65-conserved domains. Some genes were also filtered out based on variation in gene length and conserved domain length. Finally, a total of 12 *LbCCO* genes were identified in the *L. barbarum* genome (Supplemental Table S2).

To classify and identify the evolutionary relationships of the *CCO* genes in *L. Barbarum*, a maximum likelihood (ML) phylogenetic tree was constructed. The tree was constructed with 5000 ultrafast bootstrap replications using 50 *CCO* amino acid sequences of *Lycium* species (*L. Barbarum* and *L. Ruthenicum*), model plants (*Solanum lycopersicum*, *Arabidopsis thaliana*, and *Nicotiana tabacum*), and *Crocus sativus* (Figure 1). Other than the *LbCCOs*, these *CCO* genes were previously identified and documented in the NCBI database. All *CCO* genes were classified into seven subfamilies including *NCED*, *CCD1*, *CCD2*, *CCD3*, *CCD4*, *CCD7*, and *CCD8* based on the similarity and homology of amino acid sequences. The *CCD3* subfamily was the first discovered, and this subfamily clustered near *CCD1* and *CCD2*. *LbCCOs* were designated according to the relationships in the phylogeny tree with three *NCEDs*, one *CCD1*, two *CCD3s*, three *CCD4s*, one *CCD7*, and one *CCD8* identified in the *L. barbarum* genome.

3.2. Physicochemical Properties, Subcellular Localization Prediction, and Function Prediction of LbCCOs

Physicochemical properties of the identified *L. barbarum* *CCOs* were predicted using amino acid sequences. Protein length, MW (molecular weight), pI (isoelectric point), instability index, aliphatic index, and GRAVY (grand average of hydropathicity) were calculated by ExPASy-ProtParam. The amino acid lengths of *LbCCOs* ranged from 506 aa (*LbNCED6-2*) to 1105 aa (*LbCCD4-2*). The predicted molecular weights ranged from 60.0 kDa (*LbNCED6-2*, *LbNCED1*) to 123.4 kDa (*LbCCD4-3*, *LbNCED6-1*). The predicted pI values of *LbCCOs* ranged from 5.54 (*LbNCED6-2*) to 8.55 (*LbCCD4-2*). The predicted pI values of *LbCCD1* and *LbCCD4* were greater than 7, indicating that these may be basic proteins. The predicted instability index values of *LbCCOs* ranged from 29.6 (*LbCCD8*) to 43.9 (*LbNCED6-1*), and the predicted instability index values of *LbNCED6-1*, *LbCCD7*, and *LbNCED2* were greater than 40, indicating that these are likely unstable proteins. The predicted aliphatic index values ranged from 75.8 (*LbNCED1*) to 89.67 (*LbCCD3-2*). The predicted GRAVY values of *LbCCOs* ranged from -0.403 (*LbNCED1*) to -0.179 (*LbCCD4-2*), and all were less than 0, indicating all *LbCCOs* are likely hydrophilic proteins. The subcellular localization prediction of *LbCCOs* was conducted by TargetP-2.0, and the result showed that *LbCCD4s* and *LbNCED6-1* can localize to chloroplasts, and the other *LbCCOs* map to the cytoplasm. Detailed information is displayed in Table 1.

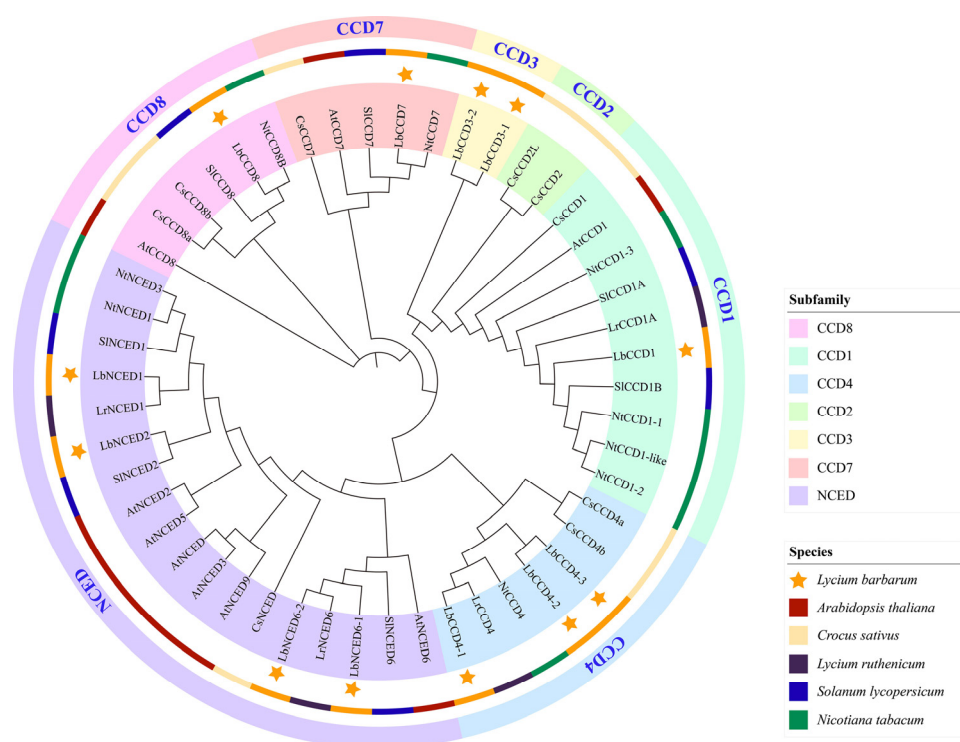


Figure 1. Phylogenetic tree of CCO protein family from *L. barbarum*, *N. tabacum*, *A. thaliana*, *S. lycopersicum*, *Crocus sativus*, and *L. ruthenicum*. A maximum likelihood (ML) phylogenetic tree was constructed by Tbttools with Auto model and 5000 ultrafast bootstraps. Similar names of CCO gene were distinguished by different colors of background and edges. Same species were exhibited in same color of stripes. Stars indicate CCOs identified in *L. barbarum*. Detailed information of all CCO proteins is listed in Supplemental Table S3.

Table 1. Predicted physiochemical properties of LbCCO proteins.

Gene Symbol	Gene ID	Protein Length (aa)	MW (kDa)	pI	Instability Index	Aliphatic Index	GRAVY	Subcellular Localization
<i>LbCCD1</i>	Lba06g01133	918	73.0	8.11	31.35	79.72	−0.250	Cytoplasm
<i>LbCCD3-1</i>	Lba04g01414	713	102.9	6.47	35.65	78.16	−0.278	Cytoplasm
<i>LbCCD3-2</i>	Lba06g00016	640	67.5	6.19	35.18	89.67	−0.189	Cytoplasm
<i>LbCCD4-1</i>	Lba04g00945	599	73.0	6.38	39.83	79.12	−0.250	Chloroplast
<i>LbCCD4-2</i>	Lba09g02158	1105	62.2	8.55	36.81	81.80	−0.179	Chloroplast
<i>LbCCD4-3</i>	Lba09g02160	539	123.4	6.16	36.73	79.78	−0.233	Chloroplast
<i>LbCCD7</i>	Lba06g02264	643	102.9	6.27	41.15	77.60	−0.372	Cytoplasm
<i>LbCCD8</i>	Lba04g01421	556	62.2	6.37	29.60	82.07	−0.343	Cytoplasm
<i>LbNCED1</i>	Lba11g00562	607	60.0	6.31	38.76	75.80	−0.403	Chloroplast
<i>LbNCED2</i>	Lba09g01724	557	72.6	6.20	41.94	82.03	−0.364	Cytoplasm
<i>LbNCED6-1</i>	Lba05g00348	587	123.4	6.48	43.90	84.48	−0.330	Chloroplast
<i>LbNCED6-2</i>	Lba05g00350	506	60.0	5.54	38.83	84.33	−0.303	Cytoplasm

3.3. Analysis of Gene Structure and Cis-Acting Elements of the LbCCOs

A motif is a similar 3D structure conserved among different proteins that serves a similar function [46]. Domains are parts of a protein with specific functions and usually move or function independently of the rest of the protein [41]. Gene structure and the conserved domains and motifs were further analyzed, and a ML phylogenetic tree was constructed with the identified LbCCOs and the CCOs from different species. Proteins from the same subfamily were clustered in one category, indicating the conservation of CCOs. The analysis of phylogeny, motifs (Figure 2A,B), domains (Figure 2C), and gene structure (Figure 2D) by Tbttools indicated similarities and differences among LbCCOs [38].

There were 3~19 and 3~10 conserved motifs and non-duplicate motifs, respectively, in the LbCCOs. One or two RPE65 domains were found in all LbCCOs. The N-terminal sequences were relatively conserved, and the most common N-terminus multi-motif was motif 4, motif 9, and motif 10. LbCCD1, LbCCD3s, LbCCD4s, and LbNCEDs were more similar than LbCCD7 or LbCCD8 subfamilies. LbCCD3s differed from LbCCD1, LbCCD4s, and LbNCEDs in the number and the type of conserved motifs. There were at least nine non-duplicate motifs in LbCCD1, LbCCD4s, and LbNCEDs, but fewer in LbCCD3s, especially in LbCCD8 and LbCCD7. LbCCD7, LbCCD8, and LbCCD3s were also distinguished from other LbCCOs by the absence of the multi-motif of motif 1, motif 8, motif 6, motif 5, motif 10, and motif 3. *LbNCEDs*, but not *LbCCDs*, possess highly conserved gene structures, motif types and locations, and numbers of conserved domains. There was more variation in the conserved motifs of LbCCDs than in LbNCEDs. Only one RPE65 domain was identified in LbNCEDs, with one or two in LbCCDs. There was no intron found in *LbNCEDs*, but there were 1~4 in *LbCCD4s*, 5~6 in *LbCCD7* and *LbCCD8*, and 12~24 in *LbCCD1* and *LbCCD3s*.

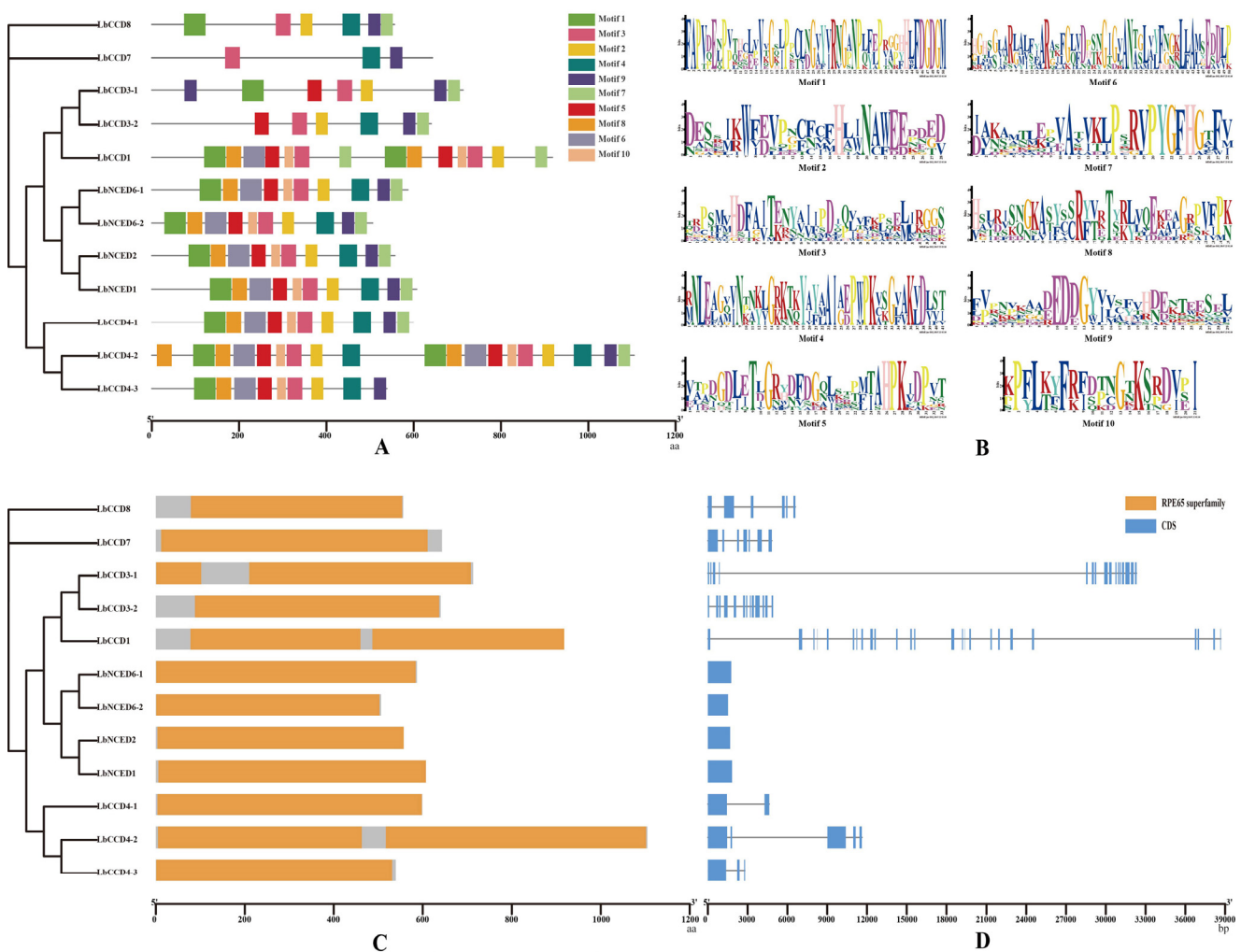


Figure 2. *LbCCOs* gene structure and cis-acting elements analysis with ML phylogenetic tree of LbCCO proteins. (A) Ten motifs were found in the LbCCOs whose sequence logos are shown in (B) of LbCCO proteins analyzed by Tbttools. (C) Conserved domain of LbCCOs. The portion without RPE65 domain of each protein was indicated in color gray. (D) CDS and intron organization of *LbCCOs*. There is an intron between the two CDS of each gene.

To investigate the potential regulation of *LbCCOs*, 2000 bp sequences upstream of the ATG translation start site of *LbCCOs* were extracted as promoter regions from the *L. barbarum* genome, and then the PlantCARE database was used to predict *cis*-acting

elements. A total of 35 *cis*-acting elements were discovered with potential environmental- and hormonal-response capabilities (Figure 3A). Environmental response elements, light, anaerobic, low-temperature, and drought response *cis*-acting elements and hormonal response elements, methyl jasmonate (MeJA), abscisic acid, salicylic acid, auxin, and gibberellin response *cis*-acting elements were found. There was considerable variation in the categories and distributions of *cis*-acting elements among *LbCCO* promoters. A statistical clustering heat map of promoter *cis*-acting elements indicated that environment changes or stresses and endogenous hormone levels are able to alter the expression of different *LbCCOs* (Figure 3B). Among all *cis*-acting elements, light-related elements, including G-box, Box 4, GT1-motif, and TCT-motif, were most abundant in the promoters of *LbCCOs*, except *LbCCD1*. This group was followed in abundance by anaerobic related elements (ARE). These elements were found in all *LbCCO* promoters except those of *LbNCED1*, *LbCCD3s*, and *LbCCD4-2*. MYB-binding sites (MBS) are related to drought response, and were found in the promoters of *LbCCD7*, *LbCCD3-2*, and *LbCCD4-3*. There were fewer MeJA response elements (CGTCA-motif and TGACG-motif) than light-related elements in *LbCCO* promoters. MeJA response elements were found in all promoters except in those of *LbNCED2* and *LbNCED4-2*. Salicylic acid related elements (TCA-elements) were only found in the promoters of *LbCCD1*, *LbCCD4-3*, and *LbCCD8*.

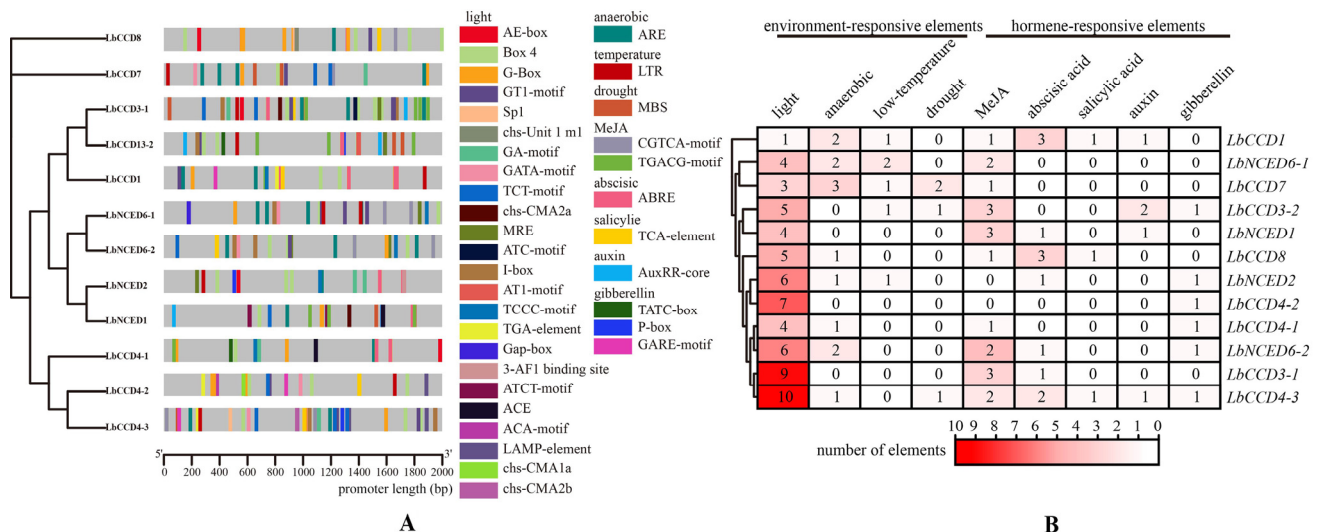


Figure 3. Prediction of *cis*-acting elements. (A) Prediction of *cis*-acting elements in the 2000 bp upstream (from the ATG) sequences of *LbCCO* promoters. The portion without *cis*-acting elements of each promoter was indicated in color gray. (B) Clustered heatmap of the number of different elements in each of hormone-responsive and environment-responsive. Darker redness indicates a larger number of specific elements in CCOs.

3.4. Chromosome Localization and Collinearity of *LbCCOs*

Collinearity analyses were conducted with the genomes of *L. barbarum*, *S. lycopersicum*, and *A. thaliana* (Figure 4). Twelve *LbCCOs* were mapped to five chromosomes of *L. barbarum*, with CCO clusters detected on chromosome 4 (*LbCCD3-1*, *LbCCD4-1*, *LbCCD8*), 5 (*LbNCED6-1*, *LbNCED6-2*), 6 (*LbCCD1*, *LbCCD3-2*, *LbCCD7*), and 9 (*LbCCD4-2*, *LbCCD4-3*). To identify whether the nearby gene is tandem, gene duplication analysis was performed of the *L. barbarum* genome using the function of one Step MCScanx in Tbttools [38]. The result showed no tandem genes for the identified *LbCCOs*. Seven *LbCCOs*, *LbNCED1*, *LbNCED2*, *LbCCD1*, *LbCCD3-1*, *LbCCD4-1*, *LbCCD7*, and *LbCCD8*, exhibited collinearity with *SICCOs* and one *LbCCO*, *LbCCD4-2*, showed collinearity with *SICCOs* and *AtCCOs*, indicating early formation. The observed collinearity was consistent with phylogeny. Compared with *L. barbarum* and *A. thaliana*, there were more collinear CCO genes between *L. barbarum* and *S. lycopersicum*, which both belong to *Solanaceae*.

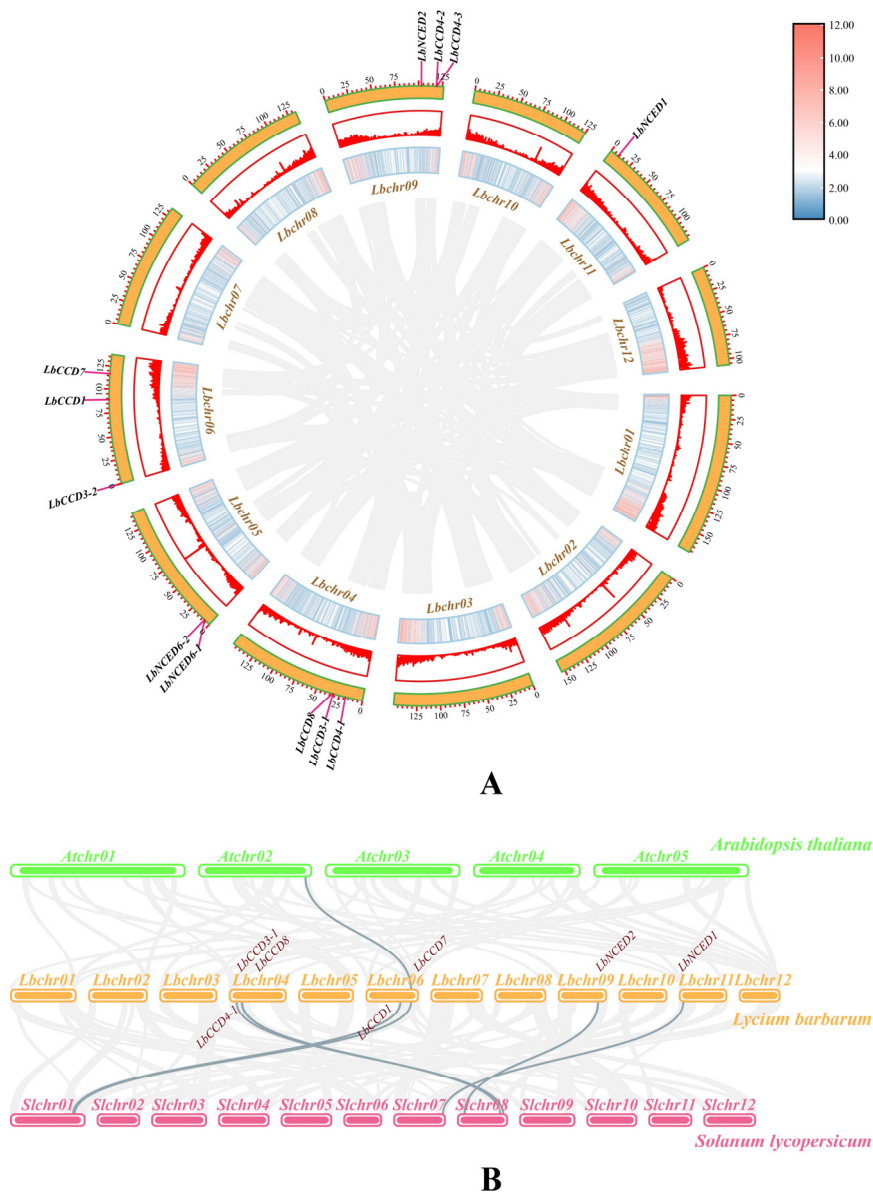


Figure 4. *LbCCOs* location and collinearity with chromosomes of *A. thaliana* and *S. lycopersicum*. (A) 12 *LbCCOs* located to five chromosomes. The scale on the outer circle is in megabases (Mb). Inner and mid-side circles show the gene density by color or column height. The connections indicate gene tandem. (B) Collinearity of chromosomes of *L. barbarum* with those of *A. thaliana* and *S. lycopersicum*. The connections indicate the relationships with collinear genes. The labelled *LbCCOs* are collinear with the CCOs linked by the darker lines in the two other species. The rest unlabeled *LbCCOs* were identified as non-collinear genes of *AtCCO* or *SlCCO*.

3.5. Expression Patterns of CCOs

CCOs are involved in carotenoid metabolism [47]. The fruit of *L. ruthenicum* has extremely low carotenoid content while that of *L. barbarum* is rich in carotenoids [35]. An analysis of gene expression was performed using RNAseq transcriptome data to identify potential differences of CCO mRNA accumulation between *L. ruthenicum* and *L. barbarum*. Three fruit development stages of green stage, turning color stage, and mature stage were analyzed, and the expression data were plotted into a clustered heat map (Figure 5B). Two expression patterns were identified by clustering clades for the three stages of fruit development. Members in clade I include *CCD4-1*, *CCD1*, and *NCED1* and showed relatively stable expression. *CCD4-1* was the most highly expressed gene among all the CCO members.

Interestingly, its expression increased during the fruit maturation process of *L. ruthenicum* but decreased rapidly in that of *L. barbarum*. *CCD1* and *NCED1* were expressed at relatively stable levels in both goji species throughout the fruit maturation process. The remaining CCOs were clustered into an unstable expression clade (clade II). *CCD4-2* seems to exhibit a similar expression pattern as *CCD4-1*, with lower expression in *L. barbarum* and greater expression in *L. ruthenicum* during fruit development. Other CCOs showed relatively low expression levels (max TPM < 3) during fruit development in the two species, except the expression of *NCED2* during the green fruit stage in *L. barbarum*. A comparison of the expression patterns of all CCOs between the two species indicates that *CCD4-1* is likely the key gene that acts to decrease carotenoids in *L. ruthenicum* fruit.

To further investigate the expression pattern in different tissues and organisms, further transcriptome analysis was conducted (Figure 5C). Two clades indicated clustering of different patterns. Clade I, including *NCED1*, *CCD1*, *CCD4-1*, and *CCD4-2*, was expressed in a more stable manner than other CCOs with expression in every organ or tissue in both goji species. Only *CCD4-2* showed lower accumulation in the mature fruit of *L. barbarum*. *CCD1* exhibited higher expression in tissues of pistils, leaves, and stem tips. The highest expressed gene of CCO was *CCD4-1*, which was found in all organs and tissues, especially in leaves and fruits, in both two *Lycium* species. The lower expression levels of *CCD4-1* were only observed in mature fruit and young *L. ruthenicum* leaves of *L. barbarum*. The expression levels of *CCD4-2* and *NCED1* were lower than those of *CCD1* or *CCD4-1*. Clade II included *NCED2*, *NCED6s*, *CCD3s*, *CCD4-3*, *CCD7*, and *CCD8*. *NCED6s* showed preferred expression in stamens, pistils, and green fruit, with trace amounts in the *L. ruthenicum* stem tip. *NCED2* showed preferred expression in *L. barbarum* stamens and *L. ruthenicum* pistils. The remaining CCOs in Clade II exhibited low expression levels.

The CCO gene family is a family that negatively regulates carotenoids, and its expression abundance would be higher in *L. ruthenicum*, which is a species with hardly any carotenoid content compared with *L. barbarum* and other goji species. To further investigate how CCOs respond to salt and saline-alkali in a clearer way, the expression patterns of CCOs in *L. ruthenicum* leaves were analyzed following salt (300 mM Na⁺) and saline-alkali (300 mM Na⁺, pH = 9) treatments (Figure 5D). Based on the expression patterns, the genes were classified into two clades. Genes in clade I, including *LrCCD4-1*, *LrCCD4-2*, *LrCCD1*, and *LrNCED1*, showed significantly higher expression abundance than those in clade II, where some genes were completely unexpressed, or expressed at trace levels. Only *LrNCED1* was upregulated by the two kinds of treatments, and the expression under saline-alkaline conditions was obviously higher compared to that under salt conditions alone.

Expression patterns of the *LbCCOs* in the green and mature fruits of the *L. barbarum* in Yinchuan (in Ningxia province) and Nomhon (in Qinghai province) were investigated next (Figure 5E). The results showed that *LbCCD1* and *LbNCED1*, belonging to clade I, exhibited high expression levels. *LbCCD1* was stably expressed during the ripening process of *L. barbarum*, while the expression of *LbNCED1* decreased as the fruit ripened in both locations. The expression levels of these two genes in the fruit from Nomhon were significantly higher than those in fruit from Yinchuan. The average high and low temperature, hours of daylight and twilight, average daily incident shortwave solar energy, and other weather information were recorded in Nomhon and Yinchuan. In Nomhon, the average daily high temperature was above 19 °C; the hottest month of the year was July, with an average high of 23 °C and low of 12 °C; the average daily incident shortwave energy per square meter was above 7.1 kWh; the brightest month of the year was June, with an average of 8.0 kWh. In Yinchuan, the average daily high temperature was above 23 °C; the hottest month of the year was July, with an average high of 29 °C and low of 19 °C; the average daily incident shortwave energy per square meter was above 6.3 kWh; the brightest month of the year was June, with an average of 7.2 kWh. Given that the primary differences between the two locations are light and temperature, this suggests

that conditions of intense light irradiation and high temperature may influence the gene expression levels of *LbCCD1* and *LbNCED1*.

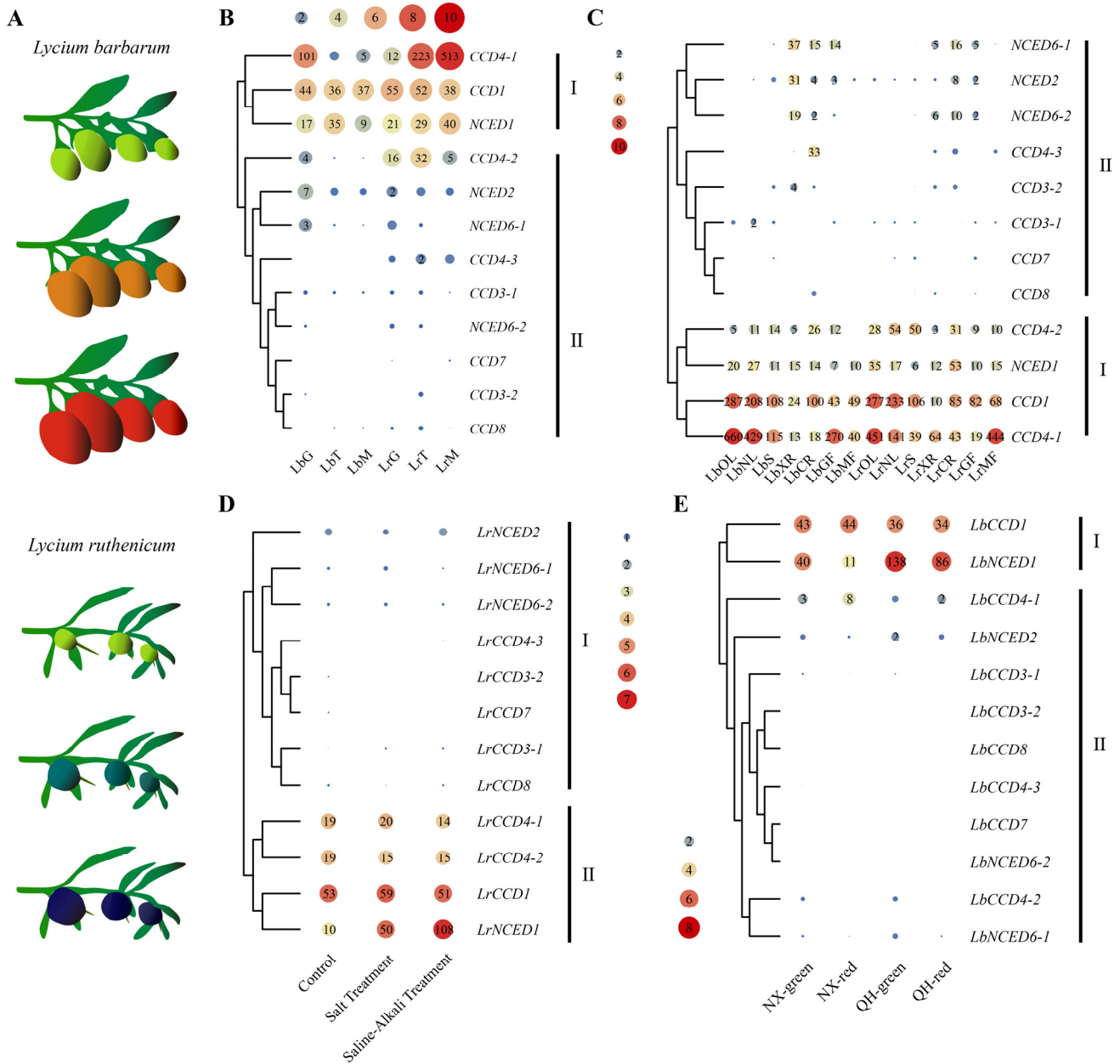


Figure 5. Fruit color changing pattern (A) and CCO expression pattern clustered heatmap (B–E); (B) clustered heat map of CCOs expression pattern of *L. barbarum* (Lb) and *L. ruthenicum* (Lr) fruit at green stage (G), turning color stage (T), and mature stage (M); (C) clustered CCOs express pattern at stamens (XR), pistils (CR), green fruits (GF), mature fruits (MF), leaves on current year branches (NL), leaves on last year branches (OL), stem tip (S) of *L. barbarum* (Lb) and *L. ruthenicum* (Lr); (D) clustered heat map of *LrCCOs* expression pattern at leaves of *L. ruthenicum* in salt and saline-alkali stress; (E) clustered heat map of *LbCCOs* expression pattern at green and red fruits of *L. barbarum* plant in Yinchuan (NX) and Nomhon (QH). The circle color and size, which were based on scaled TPM values, were used to illustrate the expression abundance, the numbers in circle of legend are scaled TPM values while the numbers in the circle of the panel are TPM values (no number is displayed for TPM value < 2). The vertical lines and groupings on the right side of the panel are clusters of genes with different expression profiles.

3.6. *CCD4-1s* Localization and Promoter Analysis of Two *Goji* Species

Given the strikingly different expression pattern for *CCD4-1s* in the two *goji* species, the *CCD4-1s* genes and their promoters were cloned and sequenced. The results showed a high similarity in both the coding areas and promoter regions. Only one amino acid varied between the two *CCD4-1* proteins (Supplemental Table S4). Subcellular localization showed that driven by the 35S promoter, both two *CCD4-1* proteins that fused to the EGFP protein were targeted to chloroplasts (Figure 6), suggesting that this single difference in the coding sequences does not affect the function of *CCD4-1*.

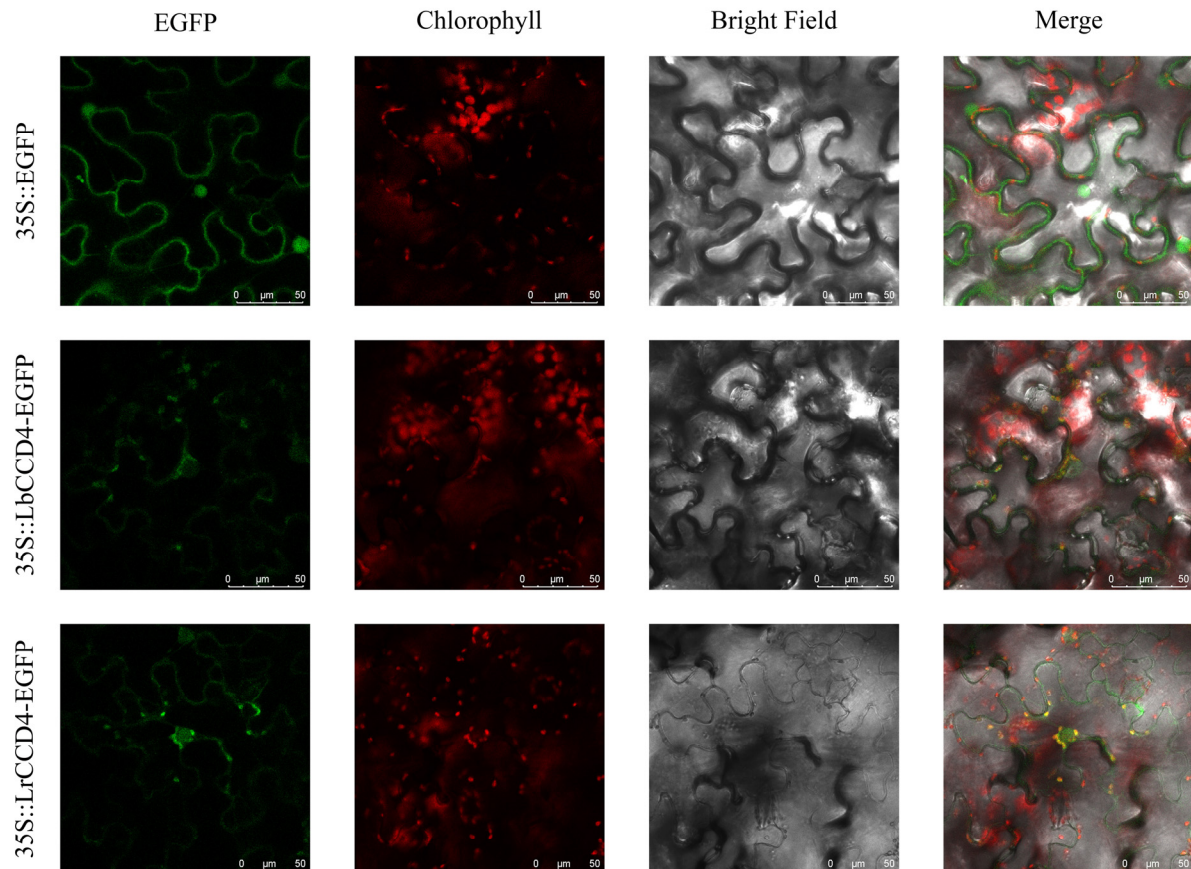


Figure 6. Subcellular localization of LbCCD4-1 and LrCCD4-1 protein. LbCCD4-1-EGFP and LrCCD4-1 fusion proteins driven by the 35S promoter were transiently expressed in tobacco epidermal cells. Images were observed by laser confocal microscopy. Scale bar = 50 μm .

To predict whether transcription factors can influence the regulation of *CCD4-1s*, binding site predictions were compared for the two *CCD4-1* promoters. The result indicated that 265 and 272 TFBS (transcription factor binding sites) exist in the promoters of *LbCCD4-1* and *LrCCD4-1*, respectively. The numbers of AP2, B3, BBR-BPC, Dof, MIKC_MADS, and NAC binding sites differed between the promoters of two *CCD4-1s*, and some of these sites may affect *CCD4-1s* expression (Table 2 and Supplemental Table S5).

Table 2. Numbers of predicted TFBS in *CCD4-1s*.

TFBS	LbCCD4-1 _{pro}	LrCCD4-1 _{pro}
AP2	11	12
ARF	1	1
ARR-B	5	5

Table 2. Cont.

TFBS	LbCCD4-1 _{pro}	LrCCD4-1 _{pro}
B3	6	9
BBR-BPC	12	13
BES1	2	2
bHLH	8	8
bZIP	7	7
C2H2	14	14
C3H	2	2
CAMTA	2	2
CPP	3	3
Dof	42	40
EIL	2	2
ERF	26	26
G2-like	10	10
GATA	3	3
GRAS	3	3
HD-ZIP	4	4
LBD	6	6
MIKC_MADS	23	25
MYB	15	15
MYB_related	2	2
NAC	35	37
Nin-like	2	2
SBP	2	2
TCP	8	8
Trihelix	1	1
VOZ	1	1
WRKY	6	6
YABBY	1	1
SUM	265	272

4. Discussion

4.1. Different Functions Classification Prediction Based on the Identification of LbCCOs

In this study, twelve *LbCCO* genes with RPE65 conserved domains were identified based on the *L. barbarum* genome. The predicted characteristics of the encoded proteins were analyzed, including pI, molecular weight, and subcellular localization. The subcellular localization prediction and experiment showed that *LbCCOs* target the chloroplasts or the cytoplasm. *LbCCOs* may function differently due to different substrate distributions. In plants, carotenoid synthesis usually occurs in the plastids, and each type of carotenoid is synthesized and then bound to the membrane of chloroplasts [10,47,48]. According to a previous report, most *CCO* members were localized to the plastid membrane, except for *CCD1*. *CCD1* generates C13 or C14 apocarotenoids by degrading products transported outside the chloroplast that have undergone degradation by other *CCOs*, rather than by the direct degradation of C40 carotenoid substrates and producing apocarotenoids [49]. The prediction of *CCOs* showed that some *CCOs* located to the cytoplasm, perhaps by the mutation of the *CCO* chloroplast transit peptide with *CCO* evolution.

In most plant species, the *CCO* gene family includes *CCD1*, *CCD4*, *CCD7*, *CCD8*, and *NCED* subfamilies [28,37,50]. In some *Crocus* species, the *CCD2* subfamily is also included [51]. In this study, *LbCCD1*, *LbCCD3*, *LbCCD4*, *LbCCD7*, *LbCCD8*, and *LbNCED* were identified in the *L. barbarum* genome, but *LbCCD2* was not found, indicating that this kind of *CCO* may not be present in this species. We identified and named a new subfamily member, *CCD3*, in *LbCCOs*. *CCO* gene family members have been identified in many species, such as pepper [52], litchi [53], and tobacco [54], but *CCD3* was not reported in these species. However, *CCD3* may exist in other species. For example, collinear analysis indicated that *LbCCD3-1* is collinear with a gene on *S. lycopersicum* chromosome 8, and

these two genes may be orthologs. The *CCD3* subfamily may not have been identified previously because the *CCD2* subfamily in non-model plant species, such as *C. sativus*, has rarely been used to build phylogenetic trees. Although the use of a phylogenetic tree can help distinguish subfamilies among species, the result can be easily affected by the selected sequences. For example, *C. sativus* CCO proteins including *CCD2* were used to build a phylogenetic tree in this study, and the result showed that *CCD2* and *CCD1* clustered to a same clade, and then clustered with *CCD3*, which was distinguished as a new subfamily. If *CCD2* was not included in the phylogenetic tree, *CCD2* or *CCD3* could have been identified as *CCD1*. Further analysis showed that *LbCCOs* can be divided into four groups according to the motif number, type, relative position, and gene structure. Group I included *LbNCEDs*, group II included *LbCCD1* and *LbCCD4s*, group III included *LbCCD7* and *LbCCD8*, and group IV included *LbCCD3s*. Different groups may have different functions. *NCED* participated in ABA synthesis [27]. *CCD1* and *CCD4* were reported to cut a variety of carotenoid substances to produce aromas or pigments. *CCD7* and *CCD8* were related to the production, SL [47]. The functions of *CCD3* may differ from those of *CCOs* and *CCD2*, and this should be a focus of future work.

Although subfamilies of *CCOs* differed in gene structure, motif number, type, and relative position, their properties are conserved among species within the same subfamilies [8,37,50]. The mutation of key genes may cause death or abnormal development, so the high conservation of *CCOs* suggests that they play important roles in regulating plant growth, development, and reproduction. The conservation level within the *LbCCO* subfamily differed. The function of *NCEDs* is to synthesize ABA, a key hormone determining plant survival and reproduction [27], indicating that *NCEDs* are a more conserved subfamily than *CCDs*. This is consistent with the gene structure and motif analysis.

4.2. Gene Conservation and Pseudogene *LbCCOs*

Tandem duplication allows for the expansion and evolution of gene families. Additionally, the tandem duplication of *CCOs* has been found in many species [28,37]. The *Ka/Ks* ratio measures the direction and magnitude of selection [50]. Although clusters were identified, no evidence for the duplication of *LbCCOs* was found, suggesting that the use of the *Ka/Ks* ratio to analyze the contraction and expansion of this family is not informative. Some *CCOs* were identified with a vestigial or no RPE65 domain, suggesting that during the evolution of the Solanaceae, the *CCO* gene family expanded and pseudogenes were generated, leading to the loss of tandem duplicated *CCOs*. The evolution of a pseudogene can lead to its disappearance or the production of new copies [55–57]. These genes generally acquire mutations, insertions, and deletions without any apparent evolutionary pressures [58]. Collinearity analysis showed that *S. lycopersicum* shares more collinear genes with *L. barbarum* than *A. thaliana*. This result is consistent with the phylogenetic relationships, as *S. lycopersicum* and *L. barbarum* are Solanaceae plants. In *S. lycopersicum* and *L. barbarum*, at least one gene in each gene subfamily is collinear, suggesting that there may be unique functions in each *LbCCO* subfamily.

4.3. *CCD4-1* May Be a Key Gene Dominating the Degradation of Goji Carotenoids

CCOs are considered important genes for carotenoid degradation to short chain apocarotenoids [59]. Phytoene synthase (*PSY*) is rate limiting for phytoene formation in the biosynthesis of carotenoids [59]. The overexpression of *PSY* resulted in a dramatic accumulation of mainly β -carotene in roots and non-green calli in leaves of *Arabidopsis*, with a high level of C13 apocarotenoid glycoside, the product of *CCD4* cleavage carotenoid, detected in the leaves [59]. A mutant of *CCD4* indicated that the cleavage effect of *CCD4* explains the lack of excessive accumulation of carotenoids in the leaves of *PSY* overexpressing plants [59]. Overall, the results show that *CCD4* is a key gene in carotenoid metabolism in *Arabidopsis*. A previous study of *L. barbarum* genomics indicated that *CCD* (*Lba03g01270*) may be involved in carotenoid degradation [36]. *L. barbarum* and *L. ruthenicum* fruits differed significantly in carotenoid content, with *L. barbarum* rich in carotenoids in mature

fruits and *L. ruthenicum* fruits containing almost no carotenoids [35]. In this study, *CCD4-1s* (Lba04g00945) was the most highly expressed gene in both *Lycium* species, with a similar expression pattern among organs and tissues, except fruit. Transcriptome analysis showed that the expression level of *CCD4-1* dramatically increased in *L. ruthenicum* and decreased in *L. barbarum* during fruit development. This completely opposite expression pattern of CCOs in the fruits of the two *goji* species indicated that the low expression of *CCD4-1* contributed to the degradation of carotenoids, especially in *L. ruthenicum*. The previously found *CCD* (Lba03g01270) was not identified as a CCO member in this study because it lacks the RPE65 domain. *CCD4-1* rather than *CCD* (Lba03g01270) may dominate the degradation of carotenoids. By comparing the coding sequences and promoter sequences of the two *CCD4-1* genes, we found that the differences in the transcription factor binding sites rather than differences in the coding sequences of the genes may explain the different carotenoid degradation efficiencies between the two *goji* species.

4.4. Abiotic Stress May Regulate the Expressions of *CCD1*, *NCED1*, or Other CCOs Directly or through Hormones in at Least One Species of *Lycium*

Gene expression analysis indicated *LrNCED1* was the only CCO that responded to salt or saline-alkali stresses, with the upregulation of *LrNCED1* expression under treatments. The upregulation of *LrNCED1* is more significant under saline-alkaline stress compared to solely salt stress. *NCEDs* were reported to synthesize ABA [23]. The upregulated *LrNCED1* may promote plants to accumulate ABA to resist abiotic stress.

In this study, *cis*-acting elements were predicted by PlantCare with certain predictive accuracy to determine the factors that regulate *LbCCOs* expression. Among all *cis*-acting elements, light related elements were the most frequent elements found in CCO members other than *LbCCD1*, indicating that light may regulate the expression of CCOs to change the content of carotenoids and hormones. Light provides energy for plants to survive but can also cause harm to plants. Photooxidative stress conditions can induce the formation of a variety of volatile short-chain aldehydic or ketonic derivatives of β -carotene, such as β -ionone or β -cyclocitral, which can increase tolerance to photooxidative stress [60]. These products can also be produced enzymatically by CCOs [47]. Although evidence suggests that these products are not produced by CCOs under intense-light stress, the expression of CCOs may be activated by light and then influence the synthesis of these products [61]. The expression of *CCD* homologs, which may be related to retinal synthesis, increased in the microorganism *Chlorogloeopsis fritschii* under UV [62]. Light not only provides energy, but also transmits environmental signals. A study of *Vaccinium myrtillus* fruit development under different light conditions showed that the degradation of carotenoids can be influenced by light, especially red/far-red light wavelengths. Light activated the expression of *VmCCD1* and *VmNCED1*, leading to carotenoid degradation and ABA synthesis [63]. *CCD7* and *CCD8* are regulated by phyB and hy5-related pathways. As the key red (R)-light photoreceptor, phytochrome B (phyB) activates the key transcription factor, ELONGATED HYPOCOTYL5 (HY5), to regulate photomorphogenesis, root development, and response to stresses in plants. Activated HY5 acts as a crucial hub to integrate light and other signals to regulate the expression of downstream genes. Shoot phyB triggers the accumulation of shoot-derived HY5 in root, promoting the expression of *CCD7* and *CCD8* and leading to the synthesis and accumulation of strigolactone (SL) in roots [64].

In addition to light response elements, hormones and other environmental response elements were enriched in the promoters of *LbCCOs*. Hormones and environment stress treatments can alter the expression of CCOs in some plant species [52]. There are many MeJA response *cis*-acting elements in the promoters of *LbCCOs*, except *LbNCED2* and *LbCCD4-2*. MeJA treatment can activate the expression of tobacco CCOs [54]. The expression patterns of CCOs differed for different genes and in different gene subfamilies. CCOs with promoters lacking MeJA response *cis*-acting elements also respond differently to MeJA [54], suggesting the indirect regulation of MeJA. Previous studies have shown that the rapid and massive accumulation of MeJA *goji* may explain the development of heat tolerance in *goji* [65].

The CCOs have been reported to be induced by high temperature in other species, and MeJA and high temperature treatment cause some *CaCCOs* to show similar expression patterns [52], suggesting heat tolerance goji may respond to high temperature stress by regulating MeJA signal.

The expression levels of *LbCCOs* in *L. barbarum* planted in different places were investigated. The geographical difference between the Yinchuan and Nomhon goji production areas lies primarily in altitude, which affects both light and temperature. Weather data also indicated differences in temperature and solar radiation between the two places. The high temperature in Yinchuan during July and August limits goji harvesting, while the cooler temperature in Nomhon allows for continuous harvesting. The differential expression of *LbCCD1* and *LbNCED1* in these two regions may be caused by differences in light and temperature conditions. Overall, these results suggest that the regulation of the expression of *CCD1* and *NCED1* in goji fruit may be regulated by a complex signaling network triggered by differences in light and temperature.

5. Conclusions

In this study, we investigated 12 *LbCCO* genes after screening the genome of *L. barbarum*. We analyzed the physicochemical properties of the 12 *LbCCOs* and found that all proteins were predicted to be localized to the cytoplasm or chloroplasts. The phylogenetic tree constructed with related species and *Crocus sativus* classified CCOs into seven subfamilies of *NCED*, *CCD1*, *CCD2*, *CCD3*, *CCD4*, *CCD7*, and *CCD8*. *CCD3* was first identified as a subfamily to distinguish it from *CCD1* and *CCD2*. The clustering results, gene structure, and motif analysis indicated different degrees of conservation for the different *LbCCO* subfamilies, with the *LbNCED* subfamily as the most highly conserved. The analysis of the promoter elements of *CCO* genes showed that the expression of these genes could be affected by environmental and hormonal factors such as light and MeJA. This is consistent with environment responsive gene expression analysis. The transcriptomes analysis indicated that the regulation of the *CCO* gene by salt-alkali stress and photothermal conditions could occur directly or indirectly (through hormonal pathways) in at least one species of *Lycium*. Collinearity analysis did not reveal tandem duplication in the *LbCCO* gene family. However, *L. barbarum* shares at least one *CCO* gene in one subfamily with *S. lycopersicum*, indicating pseudogene generation and the importance of the different *CCO* subfamilies. The spatiotemporal transcriptome analysis revealed different expression patterns of *LbCCOs* in different tissues or organs and the fruit developmental process. *CCD4-1* showed opposite expression patterns in the fruit development process of the two *goji* species, suggesting that *LbCCD4-1* may dominate the degradation of carotenoids in *goji* fruit.

Supplementary Materials: The following supporting information can be downloaded at: <https://www.mdpi.com/article/10.3390/f14050983/s1>, Supplemental Table S1: Cloning primers; Supplemental Table S2: CDS sequence of *LbCCOs* from *L. barbarum*; Supplemental Table S3: Protein sequence of CCOs from *L. barbarum*, *N. tabacum*, *A. thaliana*, *S. lycopersicum*, *Crocus sativus*, and *L. ruthenicum*; Supplemental Table S4: Sequences Alignment of *CCD4-1s* and their promoters from *L. barbarum* and *L. ruthenicum*; Supplemental Table S5 Binding site prediction results of *CCD4-1s* promoters.

Author Contributions: Conceptualization, J.C. (Jinhuan Chen); methodology, W.L.; formal analysis, W.L. and J.C. (Jiahang Che); investigation, W.L.; data curation, J.C. (Jinhuan Chen), W.L., J.C. (Jiahang Che) and Q.L.; writing—original draft preparation, W.L.; writing—review and editing, J.C. (Jinhuan Chen), C.W. and G.D.; visualization, W.L.; project administration, J.C. (Jinhuan Chen); funding acquisition, J.C. (Jinhuan Chen) and Q.L. All authors have read and agreed to the published version of the manuscript.

Funding: This research was funded by the Key Research and Development Program of Ningxia, grant number 2021BEF02005; the Key Research and Development Program of Ningxia, grant number 2022BBF01001-02, and National College Students' Science and Technology Innovation Project: X202210022069.

Data Availability Statement: The datasets supporting the results presented in this manuscript are included within the article (and its Supplementary Materials). Raw data of *L. barbarum* and *L. ruthenicum* fruit developmental process sequenced libraries are available in the NCBI SRA database under number PRJNA483521 [<https://www.ncbi.nlm.nih.gov/sra/?term=PRJNA483521>], accessed on 20 April 2022. Raw data of stress responsive transcriptomes of *L. ruthenicum* are available in the NCBI SRA database under number PRJNA285517 [<https://www.ncbi.nlm.nih.gov/sra/?term=PRJNA285517>], accessed on 20 April 2022.

Conflicts of Interest: The authors declare no conflict of interest.

References

- Hitchcock, C.L. A Monographic Study of the Genus *Lycium* of the Western Hemisphere. *Ann. Mo. Bot. Gard.* **1932**, *19*, 179. [[CrossRef](#)]
- Nee, M. Flora of China, Vol. 17, Verbenaceae Through Solanaceae. *Brittonia* **1996**, *48*, 611. [[CrossRef](#)]
- Yu, Z.; Xia, M.; Lan, J.; Yang, L.; Wang, Z.; Wang, R.; Tao, H.; Shi, Y. A Comprehensive Review on the Ethnobotany, Phytochemistry, Pharmacology and Quality Control of the Genus *Lycium* in China. *Food Funct.* **2023**, *14*, 2998–3025. [[CrossRef](#)] [[PubMed](#)]
- Zhang, Q.; Chen, W.; Zhao, J.; Xi, W. Functional Constituents and Antioxidant Activities of Eight Chinese Native Goji Genotypes. *Food Chem.* **2016**, *200*, 230–236. [[CrossRef](#)]
- Avalos, J.; Carmen Limón, M. Biological Roles of Fungal Carotenoids. *Curr. Genet.* **2015**, *61*, 309–324. [[CrossRef](#)]
- Sun, T.; Rao, S.; Zhou, X.; Li, L. Plant Carotenoids: Recent Advances and Future Perspectives. *Mol. Hortic.* **2022**, *2*, 3. [[CrossRef](#)]
- Maoka, T. Carotenoids as Natural Functional Pigments. *J. Nat. Med.* **2020**, *74*, 1–16. [[CrossRef](#)]
- Kim, Y.; Hwang, I.; Jung, H.-J.; Park, J.-I.; Kang, J.-G.; Nou, I.-S. Genome-Wide Classification and Abiotic Stress-Responsive Expression Profiling of Carotenoid Oxygenase Genes in Brassica Rapa and Brassica Oleracea. *J. Plant Growth Regul.* **2016**, *35*, 202–214. [[CrossRef](#)]
- Lin, J.; Massonnet, M.; Cantu, D. The Genetic Basis of Grape and Wine Aroma. *Hortic. Res.* **2019**, *6*, 81. [[CrossRef](#)]
- Yuan, H.; Zhang, J.; Nageswaran, D.; Li, L. Carotenoid Metabolism and Regulation in Horticultural Crops. *Hortic. Res.* **2015**, *2*, 15036. [[CrossRef](#)]
- Lim, J.; Lim, C.W.; Lee, S.C. Core Components of Abscisic Acid Signaling and Their Post-Translational Modification. *Front. Plant Sci.* **2022**, *13*, 895698. [[CrossRef](#)]
- Waadt, R.; Seller, C.A.; Hsu, P.-K.; Takahashi, Y.; Munemasa, S.; Schroeder, J.I. Plant Hormone Regulation of Abiotic Stress Responses. *Nat. Rev. Mol. Cell Biol.* **2022**, *23*, 680–694. [[CrossRef](#)] [[PubMed](#)]
- Rehman, N.U.; Li, X.; Zeng, P.; Guo, S.; Jan, S.; Liu, Y.; Huang, Y.; Xie, Q. Harmony but Not Uniformity: Role of Strigolactone in Plants. *Biomolecules* **2021**, *11*, 1616. [[CrossRef](#)] [[PubMed](#)]
- Yoneyama, K.; Brewer, P.B. Strigolactones, How Are They Synthesized to Regulate Plant Growth and Development? *Curr. Opin. Plant Biol.* **2021**, *63*, 102072. [[CrossRef](#)] [[PubMed](#)]
- Liang, N.; Yao, M.-D.; Wang, Y.; Liu, J.; Feng, L.; Wang, Z.-M.; Li, X.-Y.; Xiao, W.-H.; Yuan, Y.-J. Cs CCD2 Access Tunnel Design for a Broader Substrate Profile in Crocetin Production. *J. Agric. Food Chem.* **2021**, *69*, 11626–11636. [[CrossRef](#)]
- Ilg, A.; Yu, Q.; Schaub, P.; Beyer, P.; Al-Babili, S. Overexpression of the Rice Carotenoid Cleavage Dioxygenase 1 Gene in Golden Rice Endosperm Suggests Apocarotenoids as Substrates in Planta. *Planta* **2010**, *232*, 691–699. [[CrossRef](#)]
- Auldrige, M.E.; Block, A.; Vogel, J.T.; Dabney-Smith, C.; Mila, I.; Bouzayen, M.; Magallanes-Lundback, M.; DellaPenna, D.; McCarty, D.R.; Klee, H.J. Characterization of Three Members of the Arabidopsis Carotenoid Cleavage Dioxygenase Family Demonstrates the Divergent Roles of This Multifunctional Enzyme Family. *Plant J.* **2006**, *45*, 982–993. [[CrossRef](#)] [[PubMed](#)]
- Cheng, L.; Huang, N.; Jiang, S.; Li, K.; Zhuang, Z.; Wang, Q.; Lu, S. Cloning and Functional Characterization of Two Carotenoid Cleavage Dioxygenases for Ionone Biosynthesis in Chili Pepper (*Capsicum annuum* L.) Fruits. *Sci. Hortic.* **2021**, *288*, 110368. [[CrossRef](#)]
- Mathieu, S.; Terrier, N.; Procureur, J.; Bigey, F.; Günata, Z. A Carotenoid Cleavage Dioxygenase from *Vitis vinifera* L.: Functional Characterization and Expression during Grape Berry Development in Relation to C13-Norisoprenoid Accumulation. *J. Exp. Bot.* **2005**, *56*, 2721–2731. [[CrossRef](#)]
- Meng, N.; Yan, G.-L.; Zhang, D.; Li, X.-Y.; Duan, C.-Q.; Pan, Q.-H. Characterization of Two *Vitis Vinifera* Carotenoid Cleavage Dioxygenases by Heterologous Expression in *Saccharomyces Cerevisiae*. *Mol. Biol. Rep.* **2019**, *46*, 6311–6323. [[CrossRef](#)]
- Rodrigo, M.J.; Alquézar, B.; Alós, E.; Medina, V.; Carmona, L.; Bruno, M.; Al-Babili, S.; Zacarías, L. A Novel Carotenoid Cleavage Activity Involved in the Biosynthesis of Citrus Fruit-Specific Apocarotenoid Pigments. *J. Exp. Bot.* **2013**, *64*, 4461–4478. [[CrossRef](#)] [[PubMed](#)]
- Ren, C.; Guo, Y.; Kong, J.; Lecourieux, F.; Dai, Z.; Li, S.; Liang, Z. Knockout of VvCCD8 Gene in Grapevine Affects Shoot Branching. *BMC Plant Biol.* **2020**, *20*, 47. [[CrossRef](#)]
- Cutler, A.J.; Krochko, J.E. Formation and Breakdown of ABA. *Trends Plant Sci.* **1999**, *4*, 472–478. [[CrossRef](#)] [[PubMed](#)]
- Martínez-Andújar, C.; Martínez-Pérez, A.; Ferrández-Ayela, A.; Albacete, A.; Martínez-Melgarejo, P.A.; Dodd, I.C.; Thompson, A.J.; Pérez-Pérez, J.M.; Pérez-Alfocea, F. Impact of Overexpression of 9-Cis-Epoxycarotenoid Dioxygenase on Growth and Gene Expression under Salinity Stress. *Plant Sci.* **2020**, *295*, 110268. [[CrossRef](#)] [[PubMed](#)]

25. González-Villagra, J.; Rodrigues-Salvador, A.; Nunes-Nesi, A.; Cohen, J.D.; Reyes-Díaz, M.M. Age-Related Mechanism and Its Relationship with Secondary Metabolism and Abscisic Acid in *Aristotelia Chilensis* Plants Subjected to Drought Stress. *Plant Physiol. Biochem.* **2018**, *124*, 136–145. [[CrossRef](#)] [[PubMed](#)]
26. Xia, H.; Wang, X.; Zhou, Y.; Su, W.; Jiang, L.; Deng, H.; Li, M.; Zhuang, Q.; Xie, Y.; Liang, D. Biochemical and Molecular Factors Governing Flesh-Color Development in Two Yellow-Fleshed Kiwifruit Cultivars. *Sci. Hortic.* **2021**, *280*, 109929. [[CrossRef](#)]
27. Noronha, H.; Silva, A.; Silva, T.; Fruscianta, S.; Diretto, G.; Gerós, H. VviRaf5 Is a Raffinose Synthase Involved in Cold Acclimation in Grapevine Woody Tissues. *Front. Plant Sci.* **2022**, *12*, 754537. [[CrossRef](#)]
28. Cai, X.; Jiang, Z.; Tang, L.; Zhang, S.; Li, X.; Wang, H.; Liu, C.; Chi, J.; Zhang, X.; Zhang, J. Genome-Wide Characterization of Carotenoid Oxygenase Gene Family in Three Cotton Species and Functional Identification of GaNCED3 in Drought and Salt Stress. *J. Appl. Genet.* **2021**, *62*, 527–543. [[CrossRef](#)]
29. Huang, Y.; Guo, Y.; Liu, Y.; Zhang, F.; Wang, Z.; Wang, H.; Wang, F.; Li, D.; Mao, D.; Luan, S.; et al. 9-Cis-Epoxycarotenoid Dioxygenase 3 Regulates Plant Growth and Enhances Multi-Abiotic Stress Tolerance in Rice. *Front. Plant Sci.* **2018**, *9*, 162. [[CrossRef](#)]
30. Toscano, S.; Trivellini, A.; Cocetta, G.; Bulgari, R.; Francini, A.; Romano, D.; Ferrante, A. Effect of Preharvest Abiotic Stresses on the Accumulation of Bioactive Compounds in Horticultural Produce. *Front. Plant Sci.* **2019**, *10*, 1212. [[CrossRef](#)]
31. da Silva Oliveira, C.E.; Zoz, T.; de Castro Seron, C.; Boleta, E.H.M.; de Lima, B.H.; Souza, L.R.R.; Pedrinho, D.R.; Matias, R.; dos Santos Lopes, C.; de Oliveira Neto, S.S.; et al. Can Saline Irrigation Improve the Quality of Tomato Fruits? *Agron. J.* **2022**, *114*, 900–914. [[CrossRef](#)]
32. Zhou, R.; Yu, X.; Li, X.; Mendanha dos Santos, T.; Rosenqvist, E.; Ottosen, C.-O. Combined High Light and Heat Stress Induced Complex Response in Tomato with Better Leaf Cooling after Heat Priming. *Plant Physiol. Biochem.* **2020**, *151*, 1–9. [[CrossRef](#)] [[PubMed](#)]
33. Zhang, R.-R.; Wang, Y.-H.; Li, T.; Tan, G.-F.; Tao, J.-P.; Su, X.-J.; Xu, Z.-S.; Tian, Y.-S.; Xiong, A.-S. Effects of Simulated Drought Stress on Carotenoid Contents and Expression of Related Genes in Carrot Taproots. *Protoplasma* **2021**, *258*, 379–390. [[CrossRef](#)]
34. Zhao, Y.-H.; Deng, Y.-J.; Wang, Y.-H.; Lou, Y.-R.; He, L.-F.; Liu, H.; Li, T.; Yan, Z.-M.; Zhuang, J.; Xiong, A.-S. Changes in Carotenoid Concentration and Expression of Carotenoid Biosynthesis Genes in *Daucus Carota* Taproots in Response to Increased Salinity. *Horticulturae* **2022**, *8*, 650. [[CrossRef](#)]
35. Islam, T.; Yu, X.; Badwal, T.S.; Xu, B. Comparative Studies on Phenolic Profiles, Antioxidant Capacities and Carotenoid Contents of Red Goji Berry (*Lycium barbarum*) and Black Goji Berry (*Lycium ruthenicum*). *Chem. Cent. J.* **2017**, *11*, 59. [[CrossRef](#)] [[PubMed](#)]
36. Cao, Y.-L.; Li, Y.; Fan, Y.-F.; Li, Z.; Yoshida, K.; Wang, J.-Y.; Ma, X.-K.; Wang, N.; Mitsuda, N.; Kotake, T.; et al. Wolfberry Genomes and the Evolution of *Lycium* (Solanaceae). *Commun. Biol.* **2021**, *4*, 671. [[CrossRef](#)] [[PubMed](#)]
37. Chen, H.; Zuo, X.; Shao, H.; Fan, S.; Ma, J.; Zhang, D.; Zhao, C.; Yan, X.; Liu, X.; Han, M. Genome-Wide Analysis of Carotenoid Cleavage Oxygenase Genes and Their Responses to Various Phytohormones and Abiotic Stresses in Apple (*Malus domestica*). *Plant Physiol. Biochem.* **2018**, *123*, 81–93. [[CrossRef](#)]
38. Chen, C.; Chen, H.; Zhang, Y.; Thomas, H.R.; Frank, M.H.; He, Y.; Xia, R. TBtools: An Integrative Toolkit Developed for Interactive Analyses of Big Biological Data. *Mol. Plant* **2020**, *13*, 1194–1202. [[CrossRef](#)]
39. Letunic, I.; Khedkar, S.; Bork, P. SMART: Recent Updates, New Developments and Status in 2020. *Nucleic Acids Res.* **2021**, *49*, D458–D460. [[CrossRef](#)]
40. Letunic, I.; Bork, P. 20 Years of the SMART Protein Domain Annotation Resource. *Nucleic Acids Res.* **2018**, *46*, D493–D496. [[CrossRef](#)]
41. Lu, S.; Wang, J.; Chitsaz, F.; Derbyshire, M.K.; Geer, R.C.; Gonzales, N.R.; Gwadz, M.; Hurwitz, D.I.; Marchler, G.H.; Song, J.S.; et al. CDD/SPARCLE: The Conserved Domain Database in 2020. *Nucleic Acids Res.* **2020**, *48*, D265–D268. [[CrossRef](#)] [[PubMed](#)]
42. The UniProt Consortium; Bateman, A.; Martin, M.-J.; Orchard, S.; Magrane, M.; Agivetova, R.; Ahmad, S.; Alpi, E.; Bowler-Barnett, E.H.; Britto, R.; et al. UniProt: The Universal Protein Knowledgebase in 2021. *Nucleic Acids Res.* **2021**, *49*, D480–D489. [[CrossRef](#)]
43. Berardini, T.Z.; Reiser, L.; Li, D.; Mezheritsky, Y.; Muller, R.; Strait, E.; Huala, E. The Arabidopsis Information Resource: Making and Mining the “Gold Standard” Annotated Reference Plant Genome: Tair: Making and Mining the “Gold Standard” Plant Genome. *Genesis* **2015**, *53*, 474–485. [[CrossRef](#)] [[PubMed](#)]
44. Wilkins, M.R.; Gasteiger, E.; Bairoch, A.; Sanchez, J.-C.; Williams, K.L.; Appel, R.D.; Hochstrasser, D.F. Protein Identification and Analysis Tools in the ExpASY Server. In *2-D Proteome Analysis Protocols*; Humana Press: Totowa, NJ, USA, 1998; Volume 112, pp. 531–552, ISBN 978-1-59259-584-6.
45. Wang, C.; Dong, Y.; Zhu, L.; Wang, L.; Yan, L.; Wang, M.; Zhu, Q.; Nan, X.; Li, Y.; Li, J. Comparative Transcriptome Analysis of Two Contrasting Wolfberry Genotypes during Fruit Development and Ripening and Characterization of the LrMYB1 Transcription Factor That Regulates Flavonoid Biosynthesis. *BMC Genom.* **2020**, *21*, 295. [[CrossRef](#)]
46. Bailey, T.L.; Johnson, J.; Grant, C.E.; Noble, W.S. The MEME Suite. *Nucleic Acids Res.* **2015**, *43*, W39–W49. [[CrossRef](#)] [[PubMed](#)]
47. Hou, X.; Rivers, J.; León, P.; McQuinn, R.P.; Pogson, B.J. Synthesis and Function of Apocarotenoid Signals in Plants. *Trends Plant Sci.* **2016**, *21*, 792–803. [[CrossRef](#)]
48. Othman, R.; Mohd Zaifuddin, F.A.; Hassan, N.M. Carotenoid Biosynthesis Regulatory Mechanisms in Plants. *J. Oleo Sci.* **2014**, *63*, 753–760. [[CrossRef](#)]
49. Floss, D.S.; Walter, M.H. Role of Carotenoid Cleavage Dioxygenase 1 (CCD1) in Apocarotenoid Biogenesis Revisited. *Plant Signal. Behav.* **2009**, *4*, 172–175. [[CrossRef](#)]

50. Zhao, J.; Li, J.; Zhang, J.; Chen, D.; Zhang, H.; Liu, C.; Qin, G. Genome-Wide Identification and Expression Analysis of the Carotenoid Cleavage Oxygenase Gene Family in Five Rosaceae Species. *Plant Mol. Biol. Rep.* **2021**, *39*, 739–751. [[CrossRef](#)]
51. Frusciante, S.; Diretto, G.; Bruno, M.; Ferrante, P.; Pietrella, M.; Prado-Cabrero, A.; Rubio-Moraga, A.; Beyer, P.; Gomez-Gomez, L.; Al-Babili, S.; et al. Novel Carotenoid Cleavage Dioxygenase Catalyzes the First Dedicated Step in Saffron Crocin Biosynthesis. *Proc. Natl. Acad. Sci. USA* **2014**, *111*, 12246–12251. [[CrossRef](#)]
52. Yao, Y.; Jia, L.; Cheng, Y.; Ruan, M.; Ye, Q.; Wang, R.; Yao, Z.; Zhou, G.; Liu, J.; Yu, J.; et al. Evolutionary Origin of the Carotenoid Cleavage Oxygenase Family in Plants and Expression of Pepper Genes in Response to Abiotic Stresses. *Front. Plant Sci.* **2022**, *12*, 792832. [[CrossRef](#)] [[PubMed](#)]
53. Yue, X.-Q.; Zhang, Y.; Yang, C.-K.; Li, J.-G.; Rui, X.; Ding, F.; Hu, F.-C.; Wang, X.-H.; Ma, W.-Q.; Zhou, K.-B. Genome-Wide Identification and Expression Analysis of Carotenoid Cleavage Oxygenase Genes in Litchi (*Litchi Chinensis* Sonn.). *BMC Plant Biol.* **2022**, *22*, 394. [[CrossRef](#)] [[PubMed](#)]
54. Zhou, Q.; Li, Q.; Li, P.; Zhang, S.; Liu, C.; Jin, J.; Cao, P.; Yang, Y. Carotenoid Cleavage Dioxygenases: Identification, Expression, and Evolutionary Analysis of This Gene Family in Tobacco. *IJMS* **2019**, *20*, 5796. [[CrossRef](#)]
55. Dobeš, C.H.; Mitchell-Olds, T.; Koch, M.A. Extensive Chloroplast Haplotype Variation Indicates Pleistocene Hybridization and Radiation of North American *Arabidrum Drummondii*, *A. × Divaricarpa*, and *A. Holboellii* (Brassicaceae): Pleistocene HYBRIDIZATION OF ARABIS SPECIES. *Mol. Ecol.* **2004**, *13*, 349–370. [[CrossRef](#)] [[PubMed](#)]
56. Koch, M.A.; Dobeš, C.; Kiefer, C.; Schmickl, R.; Klimeš, L.; Lysak, M.A. Supernetwork Identifies Multiple Events of Plastid TrnF(GAA) Pseudogene Evolution in the Brassicaceae. *Mol. Biol. Evol.* **2007**, *24*, 63–73. [[CrossRef](#)]
57. Koch, M.A.; Dobeš, C.; Matschinger, M.; Bleeker, W.; Vogel, J.; Kiefer, M.; Mitchell-Olds, T. Evolution of the TrnF(GAA) Gene in Arabidopsis Relatives and the Brassicaceae Family: Monophyletic Origin and Subsequent Diversification of a Plastidic Pseudogene. *Mol. Biol. Evol.* **2005**, *22*, 1032–1043. [[CrossRef](#)]
58. Harrison, P.M. Digging for Dead Genes: An Analysis of the Characteristics of the Pseudogene Population in the *Caenorhabditis Elegans* Genome. *Nucleic Acids Res.* **2001**, *29*, 818–830. [[CrossRef](#)]
59. Lätari, K.; Wüst, F.; Hübner, M.; Schaub, P.; Beisel, K.G.; Matsubara, S.; Beyer, P.; Welsch, R. Tissue-Specific Apocarotenoid Glycosylation Contributes to Carotenoid Homeostasis in Arabidopsis Leaves. *Plant Physiol.* **2015**, *168*, 1550–1562. [[CrossRef](#)]
60. González-Pérez, S.; Gutiérrez, J.; García-García, F.; Osuna, D.; Dopazo, J.; Lorenzo, Ó.; Revuelta, J.L.; Arellano, J.B. Early Transcriptional Defense Responses in Arabidopsis Cell Suspension Culture under High-Light Conditions. *Plant Physiol.* **2011**, *156*, 1439–1456. [[CrossRef](#)]
61. Ramel, F.; Mialoundama, A.S.; Havaux, M. Nonenzymic Carotenoid Oxidation and Photooxidative Stress Signalling in Plants. *J. Exp. Bot.* **2013**, *64*, 799–805. [[CrossRef](#)]
62. Llewellyn, C.A.; Airs, R.L.; Farnham, G.; Greig, C. Synthesis, Regulation and Degradation of Carotenoids Under Low Level UV-B Radiation in the Filamentous Cyanobacterium *Chlorogloeopsis Fritschii* PCC 6912. *Front. Microbiol.* **2020**, *11*, 163. [[CrossRef](#)] [[PubMed](#)]
63. Karppinen, K.; Zoratti, L.; Sarala, M.; Carvalho, E.; Hirsimäki, J.; Mentula, H.; Martens, S.; Häggman, H.; Jaakola, L. Carotenoid Metabolism during Bilberry (*Vaccinium myrtillus* L.) Fruit Development under Different Light Conditions Is Regulated by Biosynthesis and Degradation. *BMC Plant Biol.* **2016**, *16*, 95. [[CrossRef](#)] [[PubMed](#)]
64. Ge, S.; He, L.; Jin, L.; Xia, X.; Li, L.; Ahammed, G.J.; Qi, Z.; Yu, J.; Zhou, Y. Light-dependent Activation of HY5 Promotes Mycorrhizal Symbiosis in Tomato by Systemically Regulating Strigolactone Biosynthesis. *New Phytol.* **2022**, *233*, 1900–1914. [[CrossRef](#)] [[PubMed](#)]
65. Qin, X.; Qin, B.; He, W.; Chen, Y.; Yin, Y.; Cao, Y.; An, W.; Mu, Z.; Qin, K. Metabolomic and Transcriptomic Analyses of *Lycium barbarum* L. under Heat Stress. *Sustainability* **2022**, *14*, 12617. [[CrossRef](#)]

Disclaimer/Publisher’s Note: The statements, opinions and data contained in all publications are solely those of the individual author(s) and contributor(s) and not of MDPI and/or the editor(s). MDPI and/or the editor(s) disclaim responsibility for any injury to people or property resulting from any ideas, methods, instructions or products referred to in the content.